2021 China Automation Congress (CAC) | 978-1-6654-2647-3/21/$31.00 ©2021 IEEE | DOI: 10.1109/CAC53003.2021.9728345

Station-keeping of Halo Orbits using Convex Optimization-Based Receding Horizon Control

Bin Zhang
Beijing Institute of Control Engineering
China Academy of Space Technology
Beijing China, 100190
Email: zbin13@buaa.edu.cn

Chao Li
Beijing Institute of Control Engineering
China Academy of Space Technology
Beijing China, 100190
Email: lichao0505@163.com

Jing Zhou
Beijing Institute of Aerospace
Systems Engineering
China Academy of Launch
Vehicle Technology
Beijing China, 100076
Email: zhoujing_bice@126.com

***Abstract*—In this work, we propose a convex optimization-based receding horizon control method for the station-keeping control of halo orbit in Earth-Moon system. we leverage the advantages of convex optimization and receding horizon control and design the method under the high-fidelity ephemeris model, making it feasible to actual mission. Simulation results show that our method reaches low tracking errors and control consumption and produces better performances than linear quadratic regulation method.**

***Index Terms*—halo orbit, ephemeris model, convex optimization, receding horizon control.**

I. INTRODUCTION

Since the success of the Chinese Queqiao mission [1] to the halo orbit about the L_2 libration point of Earth-Moon system, halo orbit has drawn increasing attention from researchers. On one hand, the Earth-Moon L_2 point plays a key role in future explorations to the far side of the Moon [2], and the nearby halo orbits are ideal mission orbits for the probes; On the other hand, halo orbits exist in every three-body system, and some of them are attractive for specific deep space missions. For example, halo orbits nearby Sun-Earth L_1 point are ideal for exploring the Sun [3]; Sun-Earth L_2 point is an ideal location for space telescopes [4].

However, due to the instability of collinear libration points, halo orbits are unstable. Therefore, employing station-keeping control to maintain the spacecraft on the mission orbit is necessary in actual missions. In the past decades, researchers have done abundant work on the station-keeping control of halo orbit. Breakwell [5] firstly introduced linear quadratic regulation (LQR) to the station-keeping control of halo orbit, but they only tested the method in the simplified dynamical model, which is not feasible for actual mission. Howell and their group [6]–[8] have done plenty of work on the target shooting method for station-keeping. Misra [9] proposed a polynomial optimization-based model predictive control method for the station-keeping control of halo orbit, but they also only tested the method in simplified model and the optimization can't be solved in real-time since the computation load is heavy with a large prediction horizon. In our previous work [10], [11], we proposed a characteristic-model based adaptive control method for the station-keeping control; This method can reach a pretty high precision in tracking errors, but the control consumption is too high.

By reviewing the past literature, we conclude that a feasible station-keeping control method should be: 1) efficiency in computation; 2) able to reach high precision with low control consumption; 3) verified in high-fidelity dynamical model. In this work, we propose a convex optimization-based receding horizon control (RHC) method for the station-keeping of halo orbit in real Earth-Moon system. On one hand, convex optimization problem has some good properties [12], such as low complexity and guarantee on the convergence to an optimal. On the other hand, RHC converts the infinite horizon optimization to finite horizon optimization and introduces feedback to the open-looped optimization, thus makes the whole method robuster to uncertainties [13]. We combine the advantages of convex optimization and RHC and design the method under ephemeris model. Therefore, the proposed method is feasible for actual missions.

The remaining of the paper is organized as following: section II presents the dynamical models and the computation of reference orbit; section III gives the design of the proposed station-keeping control method; section IV presents the simulation results and analysis; section V concludes this work.

II. DYNAMICAL MODELS AND REFERENCE ORBIT

In this work, we consider two types of dynamical models, i.e. the circular restricted three-body problem (CRTBP) and the ephemeris model, both of which are the foundations for the construction of reference orbits and the controller design.

A. CRTBP

The CRTBP is a powerful tool for the analysis of the general properties of libration points. It describes the motion of a particle (i.e. the satellite in our case) with a very small mass under the gravity of two massive primaries (i.e. Earth and Moon in our case) that are in circular motion around the common center of masses [14].

For the convenience of analysis, The CRTBP is usually studied in a synodic coordinate with nondimensionalized units of mass, lenght and time:

$$[M] = M_1 + M_2, [L] = L_{12}, [T] = \left[\frac{{L_{12}}^3}{G(M_1+M_2)}\right]^{\frac{1}{2}} \tag{1}$$

where M_1 and M_2 denotes the masses of the primaries; L_{12} denotes the mean distance between the primaries; G is the gravitational constant. Using Eq. (1), the masses of the primaries are nondimensionalized as $1-\mu$ for M_1, and μ for M_2, respectively. $\mu = M_2/(M_1+M_2)$ is the mass parameter. For the Earth-Moon system, $\mu = 0.01215058561$.

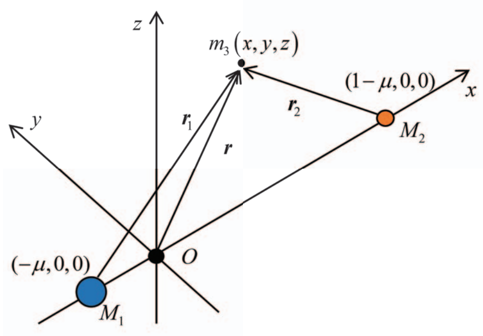

Fig. 1. Synodic coordinate

The synodic coordinate is shown in Fig.1, where M_1 and M_2 ($M_1 \geq M_2$) denote the primaries, respectively, and O is their barycenter; m_3 denotes the spacecraft; $\boldsymbol{r}$, $\boldsymbol{r}_1$, and $\boldsymbol{r}_2$ are vectors from O, M_1, and M_2 to m_3, respectively.

Let $[x,y,z]^T$ denotes the nondimensionalized position vector of the spacecraft in synodic coordinate, the equations of motion for spacecraft in CRTBP is depicted as [15]:

$$\begin{cases} \ddot{x} - 2\dot{y} = \dfrac{\partial\Omega}{\partial x} \\ \ddot{y} + 2\dot{x} = \dfrac{\partial\Omega}{\partial y} \\ \ddot{z} = \dfrac{\partial\Omega}{z} \end{cases} \tag{2}$$

where

$$\begin{cases} \Omega = \dfrac{1}{2}\left(x^2+y^2\right) + \dfrac{1-\mu}{r_1} + \dfrac{\mu}{r_2} \\ r_1 = \|\boldsymbol{r}_1\| = \left[(x+\mu)^2 + y^2 + z^2\right]^{\frac{1}{2}} \\ r_2 = \|\boldsymbol{r}_2\| = \left[(1-x-\mu)^2 + y^2 + z^2\right]^{\frac{1}{2}} \end{cases} \tag{3}$$

B. Ephemeris Model

As a simplfied model, the CRTBP is powerful for general analysis, but not feasible for actual missions. To better simulate the real dynamical environment, in this work, we introduce a high-fidelity N-body ephemeris model using the JPL DE421 [16] planetary ephemerides. By using the instantaneous positions and velocities delivered from the DE421 ephemeris data to construct the equations of motion, the ephemeris model involves the lunar eccentricity and gravitational perturbations from the Sun and other planets, thus more accurately simulates the dynamical environment.

The ephemeris model is usually constructed in inertial space rather than a rotation frame. In practice, it is more convenient to study the motion of spacecraft relative to a central body. The framework of the ephemeris model is illustrated in Fig.2.

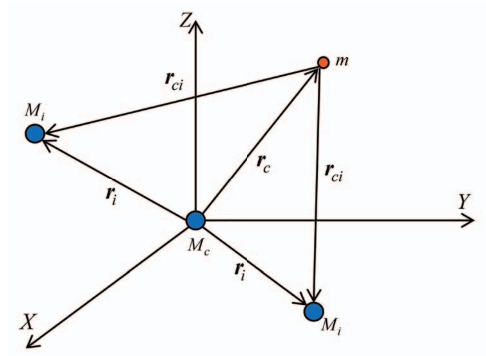

Fig. 2. The ephemeris model relative to a central body.

In Fig.2, m denotes the spacecraft; M_c and M_i denote the central body and other primaries, respectively; vector $\boldsymbol{r}_c$ denotes the position of the spacecraft respect to the central body; vector $\boldsymbol{r}_{ci}$ represents the positions of other primaries respect to the spacecraft and vector $\boldsymbol{r}_i$ represents the locations of other primaries relative to the central body. Note that vector $\boldsymbol{r}_c$ can be obtained instantaneously alongside the integration of the equations of motion and vector $\boldsymbol{r}_i$ can be delivered directly from DE421, then vector $\boldsymbol{r}_{ci}$ can be computed by $\boldsymbol{r}_{ci} = \boldsymbol{r}_i - \boldsymbol{r}_c$. Now, the equations of motion for spacecraft in the ephemeris model relative to a central body can be constructed as:

$$\ddot{\boldsymbol{r}}_c = -\frac{GM_c}{r_c^3}\boldsymbol{r}_c + \sum_{i=1}^{N-2} GM_i\left(\frac{\boldsymbol{r}_{ci}}{r_{ci}^3} - \frac{\boldsymbol{r}_i}{r_i^3}\right) \tag{4}$$

where, $r_c = \|\boldsymbol{r}_c\|$, $r_i = \|\boldsymbol{r}_i\|$, and $r_{ci} = \|\boldsymbol{r}_{ci}\|$.

Considering that this work studies the station-keeping control of halo orbit in Earth-Moon system, it's more convenient for analysis to make the Moon as the central body. Therefore, the ephemeris model constructed in the Moon-centered J2000 coordinate will be used in the following analysis and simulations.

C. Reference orbit

For the station-keeping control of halo orbit, a reference orbit is usually constructed firstly, then the spacecraft is maintained at the neighborhood of the reference orbit. There are abundant literatures on the construction of the reference orbit, and multiple shooting method is a widely-used strategy. The general idea of multiple shooting method is similar to the one used for the numerical solution of boundary-value problems [17]. Since the main focus in this work is the controller design rather than the construction of reference orbit, we simply cite the multiple shooting method proposed in Pavlak's work [18] to construct the reference orbit used in the simulations of this work. The processes of the construction of the reference orbit in ephemeris model are summarized in Table I.

TABLE I
THE PROCESS OF CONSTRUCTING THE REFERENCE ORBIT IN EPHEMERIS MODEL

Start	
Step1	Select basic parameters of halo orbit.
Step2	Obtain the approximate initial value using three order approximate solution of halo orbit.
Step3	Correct the approximate initial value using differential correction.
Step4	Converge the orbit in the CRTBP using fixed-time multiple shooting method.
Step5	Select patch points on the orbit converged in the CRTBP; dimensionalize the patch points and transit the patch points to the Moon-centered J2000 coordinate.
Step6	Nondimensionalize the patch points and reconverge the orbit in the ephemeris model using vary-time multiple shooting method.
End	

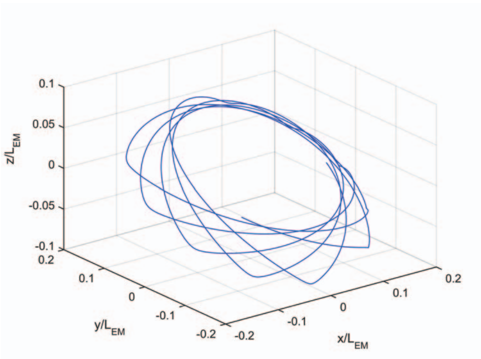

Fig. 3. Reference orbit in Moon-centered J2000 coordinate.

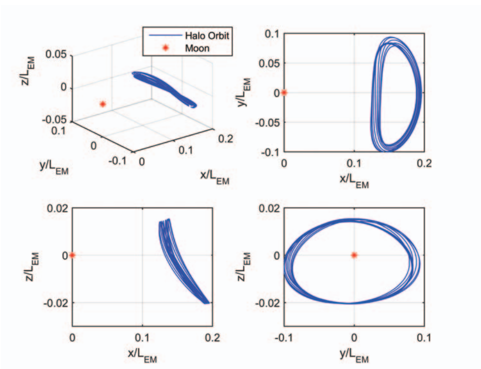

Fig. 4. Reference orbit in rotation coordinate.

In this work, we set the z-axis amplitude of the halo orbit as $A_z = 6391.5km$, and the orbit lasts 10 periods which is about 148 days. The start time of the orbit is at UTC +8, 0:00, January 1st, 2019. Employing the processes shown in Table I, we finally obtain the reference orbit used in later simulations. Fig.3 shows the reference orbit in Moon-centered J2000 coordinate and Fig.4 shows the same reference orbit in synodic coordinate.

III. CONTROLLER DESIGN

For the convenience of the later analysis, we rewrite the uncontrolled dynamical equations of the spacecraft as the following compact form:

$$\dot{\boldsymbol{X}} = f\left(\boldsymbol{X}\right) \tag{5}$$

where

$$\begin{cases} \boldsymbol{X} = \begin{bmatrix} \boldsymbol{r}_c^T & \dot{\boldsymbol{r}}_c^T \end{bmatrix}^T \\ f\left(\boldsymbol{X}\right) = \begin{bmatrix} \dot{\boldsymbol{r}}_c \\ -\frac{GM_c}{r_c^3}\boldsymbol{r}_c + \sum_{i=1}^{N-2} GM_i \left(\frac{\boldsymbol{r}_{ci}}{r_{ci}^3} - \frac{\boldsymbol{r}_i}{r_i^3}\right) \end{bmatrix} \end{cases} \tag{6}$$

Let $\boldsymbol{X}_r$ denote the reference trajectory of the spacecraft, $\boldsymbol{X}_a$ denote the actual trajectory of the spacecraft under control, we can obtain

$$\begin{cases} \dot{\boldsymbol{X}}_r = f\left(\boldsymbol{X}_r\right) \\ \dot{\boldsymbol{X}}_a = f\left(\boldsymbol{X}_a\right) + \boldsymbol{B}\boldsymbol{u}(t) \end{cases} \tag{7}$$

where

$$\begin{cases} \boldsymbol{u}(t) = \begin{bmatrix} u_1(t) & u_2(t) & u_3(t) \end{bmatrix}^T \\ \boldsymbol{B} = \begin{bmatrix} \boldsymbol{0}_{3\times3} & \boldsymbol{I}_{3\times3} \end{bmatrix} \end{cases} \tag{8}$$

$\boldsymbol{u}(t)$ is the control acceleration.

Denote $\Delta\boldsymbol{X} = \boldsymbol{X}_a - \boldsymbol{X}_r$ as the state error of the spacecraft and differentiate it, we have

$$\begin{aligned} \Delta\dot{\boldsymbol{X}} &= \dot{\boldsymbol{X}}_a - \dot{\boldsymbol{X}}_r \\ &= f\left(\boldsymbol{X}_a\right) - f\left(\boldsymbol{X}_r\right) + \boldsymbol{B}\boldsymbol{u}(t) \end{aligned} \tag{9}$$

Linearizing Eq.(9) derives

$$\Delta\dot{\boldsymbol{X}}(t) = \boldsymbol{A}(t)\Delta\boldsymbol{X}(t) + \boldsymbol{B}\boldsymbol{u}(t) \tag{10}$$

where $\boldsymbol{A}(t) = \left.\frac{\partial f(\boldsymbol{X})}{\partial \boldsymbol{X}}\right|_{\boldsymbol{X}_r}$.

A. Convex Optimization

1) Optimal control problem: In order to use the convex optimization to solve the station-keeping control problem of halo orbit, we need firstly constuct it as an optimal control problem. For the actual mission, it is important to maintain the trade-off of tracking errors and fuel consumption. Therefore, in this work, we choose the cost function of the optimization as the following form:

$$J\left(\Delta\boldsymbol{X}(t), \boldsymbol{u}(t), t\right) = \int_0^{t_f} \left(\Delta\boldsymbol{X}^T\boldsymbol{Q}\boldsymbol{X} + \boldsymbol{u}^T\boldsymbol{u}\right) dt \tag{11}$$

where $\boldsymbol{Q}$ is the weight matrix.

Now, we consider the constraints. In actual mission, the thrust for station-keeping control should be constrained. Therefore, we need to implement constraint to control input during the optimization:

$$u_{min} \leq \|\boldsymbol{u}(t)\| \leq u_{max} \tag{12}$$

where u_{min}, u_{max} are the lower boundary and upper boundary of control input, respectively, and $u_{max} > u_{min} > 0$. Besides, considering the insertion errors are inevitable when the spacecraft enters the target orbit, we should implement constraints to the initial value as well:

$$\Delta \boldsymbol{X}(0) = \Delta \boldsymbol{X}_0 \tag{13}$$

Combining Eq.(10), (11), (12), and (13), we can obtain the following optimal control problem:

$$\begin{aligned} &min \quad J\left(\Delta \boldsymbol{X}(t), \boldsymbol{u}(t), t\right) = \int_0^{t_f} \left(\Delta \boldsymbol{X}^T \boldsymbol{Q} \Delta \boldsymbol{X} + \boldsymbol{u}^T \boldsymbol{u}\right) dt \\ &S.t. \\ &\qquad \begin{cases} \Delta \dot{\boldsymbol{X}}(t) = \boldsymbol{A}(t) \Delta \boldsymbol{X}(t) + \boldsymbol{B}\boldsymbol{u}(t) \\ u_{min} \leq \|\boldsymbol{u}(t)\| \leq u_{max} \\ \Delta \boldsymbol{X}(0) = \Delta \boldsymbol{X}_0 \end{cases} \end{aligned} \tag{14}$$

2) Convexification: Note that the input constraint in Eq.(14) is a nonconvex constraint. To convert Eq.(14) to a convex optimization problem, here we introduce a slack variable $\mathfrak{U}(t)$ to do the constraint convexification. $\mathfrak{U}(t)$ and $\boldsymbol{u}(t)$ satisfy the following second-order cone constraint:

$$\begin{cases} \|\boldsymbol{u}(t)\| \leq \mathfrak{U}(t) \\ u_{min} \leq \mathfrak{U}(t) \leq u_{max} \end{cases} \tag{15}$$

After the convexification, Eq.(14) is converted to the following convex optimization problem:

$$\begin{aligned} &min \quad J\left(\Delta \boldsymbol{X}(t), \boldsymbol{u}(t), t\right) = \int_0^{t_f} \left(\Delta \boldsymbol{X}^T \boldsymbol{Q} \Delta \boldsymbol{X} + \mathfrak{U}^2\right) dt \\ &S.t. \\ &\qquad \begin{cases} \Delta \dot{\boldsymbol{X}}(t) = \boldsymbol{A}(t) \Delta \boldsymbol{X}(t) + \boldsymbol{B}\boldsymbol{u}(t) \\ \|\boldsymbol{u}(t)\| \leq \mathfrak{U}(t); u_{min} \leq \mathfrak{U}(t) \leq u_{max} \\ \Delta \boldsymbol{X}(0) = \Delta \boldsymbol{X}_0 \end{cases} \end{aligned} \tag{16}$$

3) Discretization: Problem Eq.(16) is an infinite-dimension optimization problem, which is infeasible to numerically solve. Therefore, we discretize Eq.(16) to convert it to a finite parameter optimization problem.

Let $[0, t_f]$ be the horizon of optimization and δt be the sampling time, then the horizon can be discretize as a series of time instants $t_k = k\delta t(k = 0, ..., N)$, where $t_f = N\delta t$. Employing the zero-order hold discretization, Eq.(10) can be discretized as

$$\Delta \boldsymbol{X}_k = \boldsymbol{A}_k \Delta \boldsymbol{X}_{k-1} + \boldsymbol{B}_k \boldsymbol{u}_k \tag{17}$$

where $\Delta \boldsymbol{X}_k = \Delta \boldsymbol{X}(t_k)$, $\Delta \boldsymbol{u}_k = \Delta \boldsymbol{u}(t_k)$, and

$$\begin{cases} \boldsymbol{A}_k = e^{\boldsymbol{A}(t_k)} \delta t \\ \boldsymbol{B}_k = \int_0^{\delta t} e^{\boldsymbol{A}(t_k)(\delta t - s)} \boldsymbol{B}(t_k) ds \end{cases} \tag{18}$$

Now, we obtain the final discrete convex optimization problem:

$$\begin{aligned} &min \quad J\left(\Delta \boldsymbol{X}_k, \mathfrak{U}_k, t_k\right) = \sum_{k=0}^{N} \left(\Delta \boldsymbol{X}_k^T \boldsymbol{Q} \Delta \boldsymbol{X}_k + \mathfrak{U}_k^2\right) \\ &S.t. \\ &\qquad \begin{cases} \Delta \boldsymbol{X}_k = \boldsymbol{A}_k \Delta \boldsymbol{X}_{k-1} + \boldsymbol{B}_k \boldsymbol{u}_k, k = 1, ..., N \\ \|\boldsymbol{u}_k| \leq \mathfrak{U}_k; u_{min} \leq \mathfrak{U}_k \leq u_{max} \\ \Delta \boldsymbol{X}(0) = \Delta \boldsymbol{X}_0 \end{cases} \end{aligned} \tag{19}$$

B. Receding Horizon Control

For the receding horizon control, at every time instant, we need to solve an optimization problem over a finite time horizon to get the optimal control actions and employ the first control action to the system. Let $t_h = n\delta t$ denote the time horizon and $\boldsymbol{u}^k$ the optimal solution for the optimization problem at time instant t_k, the control action at t_k is

$$\boldsymbol{u}_k = \boldsymbol{u}_0^k, k = 0, ..., n \tag{20}$$

In this work, at each time instant t_k, we solve a convex optimization problem having the form of Eq.(19) to get the control action. The resulted convex optimization-based receding horizon control law is shown in Algorithm 1.

Algorithm 1 Convex optimization-based receding horizon control

Routine

k=0

while $k < N$ **do**

1. Solve convex optimization:

$$\begin{aligned} &min \quad J\left(\Delta \boldsymbol{X}_i^k, \mathfrak{U}_i^k, t_i^k\right) = \\ &\qquad \textstyle\sum_{k=0}^{N} \left[\left(\Delta \boldsymbol{X}_i^{T k}\right)^T Q \Delta \boldsymbol{X}_i^k + \left(\mathfrak{U}_i^k\right)^2\right] \\ &S.t. \\ &\qquad \begin{cases} \Delta \boldsymbol{X}_i^k = \boldsymbol{A}_i^k \Delta \boldsymbol{X}_{i-1}^k + \boldsymbol{B}_i^k \boldsymbol{u}_i^k, i = 1, .., n \\ \|\boldsymbol{u}_i^k\| \leq \mathfrak{U}_i^k; u_{min} \leq \mathfrak{U}_i^k \leq u_{max} \\ \Delta \boldsymbol{X}_0^k = \Delta \boldsymbol{X}^k \end{cases} \end{aligned}$$

2. Implement control action $\boldsymbol{u}_k = \boldsymbol{u}_0^k$

end while

IV. Simulations

To verify the validity of the proposed convex optimization-based receding horizon control law, we implement simulation using the reference orbit constructed in Section II-C. During the simulation, the insertion errors, i.e. the initial value constraints, are set as $\Delta \boldsymbol{X}_0 = \left[\begin{array}{cc} \Delta \boldsymbol{x}_0^T & \Delta \boldsymbol{v}_0^T \end{array}\right]^T$, where:

$$\begin{cases} \Delta \boldsymbol{x}_0 = \left[\begin{array}{ccc} 38.44km & 38.44km & 38.44km \end{array}\right]^T \\ \Delta \boldsymbol{v}_0 = \left[\begin{array}{ccc} 0.1m/s & 0.1m/s & 0.1m/s \end{array}\right] \end{cases} \tag{21}$$

Besides, the sampling time is set as $\delta t = 0.01$, time horizon $t_p = 150\delta t$, weight matix $\boldsymbol{Q} = diag(3, 3, 3, 3, 3, 3)$. The convex optimization is solved though CVX, a package for specifying and solving convex programs [19], [20].

To better verify the validity of the proposed method, we employ the LQR method as a comparison. The cost function of LQR method is set as

$$J = \frac{1}{2}\int_0^{\infty}\left(\Delta \boldsymbol{X}^T \boldsymbol{Q}_1 \Delta \boldsymbol{X} + \boldsymbol{u}^T \boldsymbol{R} \boldsymbol{u}\right) dt \tag{22}$$

where $\boldsymbol{Q}_1$ and $\boldsymbol{R}$ are weight matrices:

$$\boldsymbol{Q}_1 = \begin{bmatrix} 1.25\boldsymbol{I}_{3\times3} & \boldsymbol{0}_{3\times3} \\ \boldsymbol{0}_{3\times3} & \boldsymbol{0}_{3\times3} \end{bmatrix}, \quad \boldsymbol{R} = \boldsymbol{I}_{3\times3} \tag{23}$$

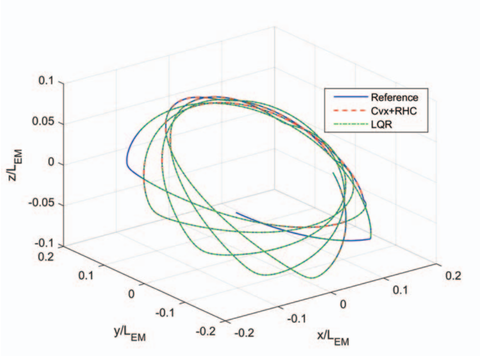

Fig. 5. The station-keeping results.

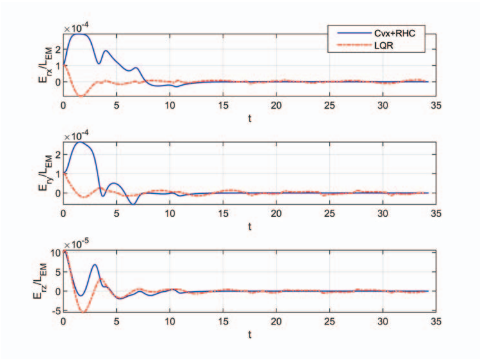

Fig. 6. The position errors.

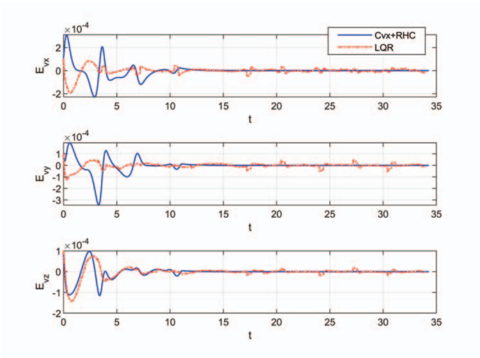

Fig. 7. The velocity errors.

The simulation results are shown in Fig.5-8. As can be seen in the graphs, the position errors and velocity errors converge

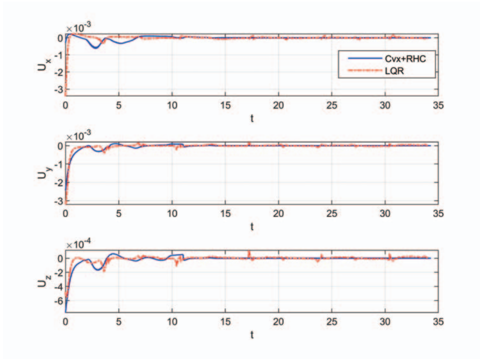

Fig. 8. The control accelerations.

to zero gradually under both methods, but LQR method has a slightly faster convergence speed than our method. The comparison of performance between the proposed method and LQR at stable stage is shown in Table II. Obviously, out proposed method out-performances the LQR method in both position errors and velocity errors. This isn't beyond expectation as our method has smoother graphs at the stable stage.

TABLE II
THE MEAN ERRORS AT STABLE STAGE

Items		X-axis	Y-axis	Z-axis
Position errors (m)	Cvx+RHC	**47.2590**	**30.1217**	**44.1854**
	LQR	1797.9	2186.6	827.7
Velocity errors ($10^{-3}m/s$)	Cvx+RHC	**0.1094**	**0.0695**	**0.0234**
	LQR	8.8	9.5	3.5

By integrating the control accelerations, we can obtain the velocity increments demanded during the simulation, as shown in Table III. Data in Table III show that the control consumption of our method is slightly larger than that of LQR method. However, when the simulation reaches the stable stage, our method demands a far more lower control consumption than LQR method. Combining the performances in tracking errors and velocity increments, our method produce better results than LQR method, thus verifies the validity of the proposed method.

TABLE III
THE VELOCITY INCREMENTS

Items		Velocity increments(m/s)
Total increments	Cvx+RHC	2.8756
	LQR	**2.8140**
Stable stage average	Cvx+RHC	**0.0021**
	LQR	0.1214

V. CONCLUSION

In this work, we propose a convex optimization-based receding horizon control law for the station-keeping control of halo orbits about the Earth-Moon L_2 libration point. Through the simulations and comparisons with LQR method, we conclude that the proposed method is feasible for the station-keeping control mission of halo orbit. The tracking errors are desirable and the demanded control consumption is low, which give the proposed method advantages in the actual missions.

REFERENCES

[1] L. Zhang, L. Xiong, J. Sun, S. Gao, X. Wang, and A. Zhang, "Technical characteristics of the relay communication satellite "queqiao" for chang'e-4 lunar farside exploration mission," *SCIENTIA SINICA Technologica*, vol. 49, no. 2, pp. 138–146, 2019.

[2] R. W. Farquhar, *The utilization of halo orbits in advanced lunar operations*. National Aeronautics and Space Administration, 1971, vol. 6365.

[3] T. Zhou, D. Li, X. Chen, and H. Yang, "Application of foreign spacecrafts of sun-earth libration points and manners of transfer trajectory," *Missiles and Space Vehicles*, vol. 5, pp. 30–34, 2004.

[4] Y. Meng, Y. Zhang, and Q. Chen, *Dynamics and control of spacecraft near libration points*. Beijing, China: Science Press, 2015, pp. 84–86.

[5] J. V. Breakwell, A. A. Kamel, and M. J. Ratner, "Station-keeping for a translunar communication station," *Celestial Mechanics*, vol. 10, no. 3, pp. 357–373, 1974.

[6] K. C. Howell and H. J. Pernicka, "Station-keeping method for libration point trajectories," *Journal of Guidance, Control, and Dynamics*, vol. 16, no. 1, pp. 151–159, 1993.

[7] T. Pavlak and K. C. Howell, "Strategy for long-term libration point orbit stationkeeping in the earth-moon system," in *Proceedings of the AAS/AIAA Astrodynamics Specialist Conference, AAS Paper*, no. 11-516, 2011.

[8] T. Pavlak and K. Howell, "Strategy for optimal, long-term stationkeeping of libration point orbits in the earth-moon system," in *AIAA/AAS Astrodynamics Specialist Conference*, 2012, p. 4665.

[9] G. Misra, H. Peng, and X. Bai, "Halo orbit station-keeping using nonlinear mpc and polynomial optimization," in *2018 Space Flight Mechanics Meeting*, 2018, p. 1454.

[10] B. Zhang and J. Zhou, "Characteristic model-based station-keeping control for halo orbit," *ACTA AERONAUTICA ET ASTRONAUTICA SINICA*, vol. 40, no. 11, p. 323206, 2019.

[11] ——, "Characteristic model-based station-keeping control for halo orbits about sun-earth l1 point," in *2019 Chinese Automation Congress (CAC)*, 2019, pp. 418–423.

[12] B. Acikmese and S. R. Ploen, "Convex programming approach to powered descent guidance for mars landing," *Journal of Guidance, Control, and Dynamics*, vol. 30, no. 5, pp. 1353–1366, 2007.

[13] D. Q. Mayne, J. B. Rawlings, C. V. Rao, and P. O. Scokaert, "Constrained model predictive control: Stability and optimality," *Automatica*, vol. 36, no. 6, pp. 789–814, 2000.

[14] G. Gomez, J. Llibre, R. Martínez, and C. Simo, *Dynamics And Mission Design Near Libration Points-Vol I: Fundamentals: The Case Of Collinear Libration Points*. Singapore: World Scientific, 2001.

[15] V. Szebehely, *Theory of orbit: The restricted problem of three Bodies*. Elsevier, 2012.

[16] W. M. Folkner, J. G. Williams, and D. H. Boggs, "The planetary and lunar ephemeris de 421," *IPN progress report*, vol. 42, no. 178, pp. 1–34, 2009.

[17] G. Gómez, J. Masdemont, and C. Simó, "Quasihalo orbits associated with libration points," *The Journal of the Astronautical Sciences*, vol. 46, no. 2, pp. 135–176, 1998.

[18] T. A. Pavlak, *Mission design applications in the earth-moon system: Transfer trajectories and stationkeeping*. Purdue University, 2010.

[19] C. R. Inc., "CVX: Matlab software for disciplined convex programming, version 2.0," http://cvxr.com/cvx, Aug. 2012.

[20] M. Grant and S. Boyd, "Graph implementations for nonsmooth convex programs," in *Recent Advances in Learning and Control*, ser. Lecture Notes in Control and Information Sciences, V. Blondel, S. Boyd, and H. Kimura, Eds. Springer-Verlag Limited, 2008, pp. 95–110, http://stanford.edu/ boyd/graph_dcp.html.